Functional reconstitution and characterization of *Pyrococcus furiosus* RNase P

Hsin-Yue Tsai*†, Dileep K. Pulukkunat†‡, Walter K. Woznick†, and Venkat Gopalan*†‡§

*Molecular, Cellular and Developmental Biology Graduate Program, ‡Ohio State Biochemistry Program, and †Department of Biochemistry, Ohio State University, Columbus, OH 43210

Communicated by Sidney Altman, Yale University, New Haven, CT, September 12, 2006 (received for review July 31, 2006)

RNase P, which catalyzes the magnesium-dependent 5′-end maturation of tRNAs in all three domains of life, is composed of one essential RNA and a varying number of protein subunits depending on the source: at least one in bacteria, four in archaea, and nine in eukarya. To address why multiple protein subunits are needed for archaeal/eukaryal RNase P catalysis, in contrast to their bacterial relative, *in vitro* reconstitution of these holoenzymes is a prerequisite. Using recombinant subunits, we have reconstituted *in vitro* the RNase P holoenzyme from the thermophilic archaeon *Pyrococcus furiosus* (*Pfu*) and furthered our understanding regarding its functional organization and assembly pathway(s). Whereas *Pfu* RNase P RNA (RPR) alone is capable of multiple turnover, addition of all four RNase P protein (Rpp) subunits to *Pfu* RPR results in a 25-fold increase in its k_{cat} and a 170-fold decrease in K_m. In fact, even in the presence of only one of two specific pairs of Rpps, the RPR displays activity at lower substrate and magnesium concentrations. Moreover, a pared-down, mini-*Pfu* RNase P was identified with an RPR deletion mutant. Results from our kinetic and footprinting studies on *Pfu* RNase P, together with insights from recent structures of bacterial RPRs, provide a framework for appreciating the role of multiple Rpps in archaeal RNase P.

archaeal RNase P | *in vitro* reconstitution | precursor tRNA processing

Ribonuclease P (RNase P) is an ancient and essential endoribonuclease that catalyzes the 5′-end maturation of tRNAs in all three domains of life (1–7). Whereas RNase P in all living organisms contains one essential RNA subunit, the number of protein cofactors/subunits varies: at least one in bacterial (8), four in archaeal (9), and nine in eukaryal (nuclear) RNase P (10, 11). The basis for this variation, which has implications for macromolecular evolution, is unclear.

The bacterial RNase P RNA (RPR) alone is catalytically active under *in vitro* conditions of high ionic strength in the presence of a divalent ion such as Mg^{2+} (1); however, the protein cofactor is essential for RNase P function *in vivo* because of its pleiotropic effects on RNA structure, substrate recognition, affinity for Mg^{2+}, and precursor tRNA (ptRNA) cleavage (12–19). Although phylogenetic sequence analysis revealed that archaeal and eukaryal RPRs likely retain the same catalytic core as the bacterial ribozyme, many archaeal and all eukaryal RPRs seem to be incapable of supporting catalysis in the absence of their protein cofactors (6, 7, 20, 21). Genetic and biochemical studies established the association of yeast/human nuclear RNase P activity with at least nine protein subunits (seven of which are homologs) (10, 11). RNase P activity could be immunoprecipitated from a partially purified *Methanothermobacter thermoautotrophicus* (*Mth*) RNase P preparation by using polyclonal antisera generated against four *Mth* polypeptides that exhibit sequence homology to four of the seven conserved yeast/human RNase P proteins (Rpps; ref. 9). None of the archaeal or eukaryal Rpps exhibit notable sequence homology to the sole bacterial Rpp (2, 5).

An essential step in understanding the individual roles of the multiple ribonucleoprotein (RNP) subunits in the archaeal/eukaryal RNase P holoenzymes is to reconstitute their activities *in vitro* and perform biochemical studies such as those performed with bacterial RNase P. Toward this goal, we chose to study RNase P from *Pyrococcus furiosus* (*Pfu*), a thermophilic archaeon, for three main reasons. First, the high sequence conservation between archaeal and eukaryal Rpps makes it likely that insights on *Pfu* RNase P assembly might be applicable to eukaryal RNase P, whose *in vitro* reconstitution has proven difficult. Second, with fewer (predicted) and smaller proteins compared with its eukaryal relatives, *Pfu* RNase P is a simpler RNP complex (one RNA and four proteins) that might possess the same catalytic RNP core present in eukaryal RNase P. Lastly, the *Pfu* Rpps are highly positively charged and thermostable, features that we expected to facilitate their purification and high-resolution structural studies, a premise that has been borne out.

Reconstitution using all or some recombinant components has been recently reported for archaeal [*Pyrococcus horikoshii* (*Pho*) and *Mth*] and eukaryal (human) RNase P (22–24). In these cases, however, the reconstituted RNase P holoenzymes displayed weak activity (compared with either their respective native versions or holoenzymes from other species) and were not fully characterized. Therefore, to establish a robust *in vitro* reconstitution system, necessary for meaningful structure-function analyses, further exploration of different sample preparation approaches or additional assay conditions are needed. The recent determination of the tertiary structures of all four archaeal Rpps (23, 25–30) lends immediacy to this objective. We now report the functional reconstitution of *Pfu* RNase P and the resulting insights into its functional organization and assembly.

Results

Approach. Although extensive biochemical characterization of partially purified native RNase P from *Mth* and *Methanococcus jannaschii* (*Mja*) has been reported (31), the protein subunit composition in these native RNase P preparations has not been established. Searches of archaeal genome sequences and results from immunoprecipitation experiments (9) support the presence of a single archaeal RPR and *at least* four Rpps (Table 2, which is published as supporting information on the PNAS web site). However, the possibility of additional Rpps in archaeal RNase P, not predicted by database mining efforts, remains until proven otherwise by elucidation of the subunit composition of a native holoenzyme. Therefore, the most logical *in vitro* reconstitution components for archaeal RNase P currently comprise its sole RPR and four Rpps.

Purification of the Recombinant Subunits of *Pfu* RNase P. *Pfu* RPR was cloned, generated by using run-off *in vitro* transcription, and

Author contributions: H.-Y.T. and D.K.P. contributed equally to this work. H.-Y.T., D.K.P., W.K.W., and V.G. designed research; H.-Y.T., D.K.P., W.K.W., and V.G. performed research; H.-Y.T., D.K.P., W.K.W., and V.G. contributed new reagents/analytic tools; H.-Y.T., D.K.P., W.K.W., and V.G. analyzed data; and H.-Y.T., D.K.P., and V.G. wrote the paper.

The authors declare no conflict of interest.

Abbreviations: *Mja*, *Methanococcus jannaschii*; *Mth*, *Methanothermobacter thermoautotrophicus*; *Pfu*, *Pyrococcus furiosus*; *Pho*, *Pyrococcus horikoshii*; ptRNA, precursor tRNA; RNP, ribonucleoprotein; Rpp, RNase P protein; RPR, RNase P RNA.

§To whom correspondence should be addressed. E-mail: gopalan.5@osu.edu.

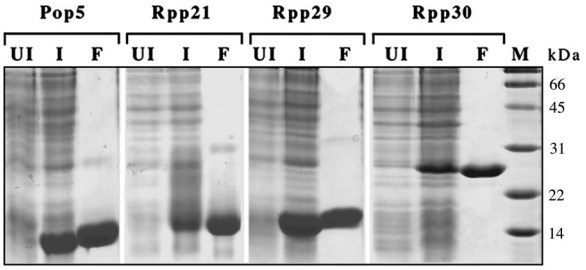

Fig. 1. SDS/PAGE analysis of the overexpression in *E. coli* and the homogeneity of the purified preparations of *Pfu* Rpps. UI and I refer to total *E. coli* crude lysates prepared from uninduced and induced cultures, respectively. F refers to the final purified preparation. M indicates molecular weight standards.

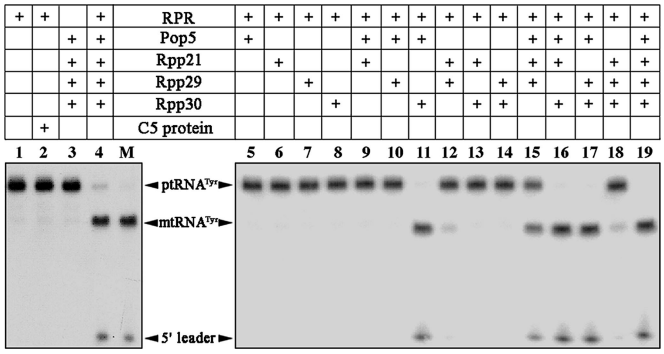

Fig. 2. Reconstitution of RNase P activity by using *Pfu* RPR and Rpps either alone or in various combinations. M refers to markers generated from processing of ptRNA^{Tyr} by *in vitro* reconstituted *E. coli* RNase P.

purified to homogeneity by using established methods (32, 33). *Pfu* Rpps were cloned, overexpressed in *Esherichia coli* BL21(DE3) Rosetta cells and purified to homogeneity by using cation-exchange and reversed-phase chromatography (Fig. 1; for details, see *Supporting Materials and Methods*, which is published as supporting information on the PNAS web site). Electrospray ionization mass spectrometry was used to verify the integrity and authenticity of the four purified *Pfu* Rpps. The molecular masses observed are in excellent agreement with those predicted by the amino acid sequences (Table 2).

***In Vitro* Reconstitution of *Pfu* RNase P.** To examine whether the putative recombinant *Pfu* Rpps could promote *Pfu* RPR function *in vitro*, we performed a standard ptRNA-processing assay (1, 32). We incubated 50 nM *Pfu* RPR and 125 nM of each *Pfu* Rpp (or C5 protein, the *E. coli* Rpp). The resulting RNPs were assayed in 50 mM Tris·HCl (pH 7.5), 30 mM $MgCl_2$, and 800 mM NH_4OAc for 2 min at 55°C with 500 nM *E. coli* ptRNA^{Tyr} as the substrate (Fig. 2, lanes 1–4). *Pfu* RPR reconstituted with its four Rpps exhibits processing of ptRNA^{Tyr} under multiple turnover conditions (Fig. 2, lanes 4 and 19). We obtain turnover numbers (k_{cat}) of 10–12 min^{-1} for the reconstituted *Pfu* RNase P; the enzyme concentration was taken to be equivalent to that of *Pfu* RPR (Table 1).

Some control experiments merit mention. First, to establish that the ptRNA-processing activity requires both the RNA and protein subunits, we performed assays with *Pfu* RPR alone (Fig. 2, lane 1) or just the four *Pfu* Rpps (Fig. 2, lane 3). Neither reaction showed any detectable activity under conditions optimal for the holoenzyme; note that the RPR alone is active at 500 mM Mg^{2+} and 2 M NH_4^+ (Fig. 5, which is published as supporting information on the PNAS web site). Second, because all four *Pfu* Rpps were purified subsequent to overexpression in *E. coli*, the remote possibility existed that the activity observed in our reconstitution studies was due to a low level contamination (undetectable by SDS/PAGE) of C5 protein (the *E. coli* Rpp), which somehow heterologously reconstituted with *Pfu* RPR. To address this caveat, we reconstituted *Pfu* RPR with highly purified recombinant C5 protein and found no ptRNA-processing activity (Fig. 2, lane 2). Finally, to ensure that the ptRNA-processing activity obtained with the reconstituted *Pfu* RNase P was not due to nonspecific cleavage, we mapped the site in ptRNA^{Tyr} that is cleaved by either the *in vitro* reconstituted *Pfu* RNase P or a partially purified preparation of native *Pfu* RNase P (Fig. 6, which is published as supporting information on the PNAS web site). Primer extension analysis of the cleaved product revealed that both reconstituted and native *Pfu* RNase P cleaved ptRNA^{Tyr} between the −1 and +1 positions, as expected for RNase P-mediated ptRNA processing (Fig. 6). Moreover, the resulting tRNA^{Tyr} possesses a 5′-phosphate as determined by analysis of RNase T2 digested products of mature tRNA^{Tyr} (Fig. 7, which is published as supporting information on the PNAS web site). Taken together, these results confirm that the enzymatic activity exhibited by the reconstituted *Pfu* RNase P is bona fide and attributable to functional reconstitution of its RNA and protein subunits.

Reconstitution of Partially and Fully Reconstituted *Pfu* RNase P. To examine whether all four proteins are needed for reconstituting an enzyme capable of multiple turnover, we assayed *Pfu* RPR (50 nM) with partial suites of the four *Pfu* Rpps (500 nM each) under multiple-turnover conditions (500 nM ptRNA^{Tyr}). The reactions were performed in 50 mM Tris·HCl (pH 7.5), 40 mM $MgCl_2$, and 800 mM NH_4OAc for 3.5 h at 55°C (Fig. 2, lanes 5–19). No RNase P activity was observed when only one *Pfu* Rpp was added to *Pfu* RPR (Fig. 2, lanes 5–8). Among the six possible two-protein combinations, only two were catalytically active: Pop5+Rpp30 and Rpp21+Rpp29 (Fig. 2, lanes 9–14). As expected from the pair-wise combination results, all four three-protein combinations display activity when reconstituted with *Pfu* RPR (Fig. 2, lanes 15–18). These data suggest that the *Pfu* RNase P holoenzyme can be built by using two initiating RNPs, either RPR+Pop5+Rpp30 or RPR+Rpp21+Rpp29 as the minimal functional complexes with the former being more active (Fig. 2, lanes 11 and 12).

Table 1. Steady-state kinetics parameters for processing of *E. coli* ptRNA^{Tyr} by partially and fully reconstituted *Pfu* RNase P holoenzymes

Reconstituted *Pfu* RNase P tested	Optimal [Mg^{2+}], mM	k_{cat}, min^{-1}	K_m, μM	k_{cat}/K_m, $M^{-1}·s^{-1}$
RPR	500	0.38 ± 0.04	30.5 ± 2.30	2.1×10^2
RPR+Rpp21+Rpp29	120	0.61 ± 0.14	6.53 ± 0.94	1.6×10^3
RPR+Pop5+Rpp30	120	11.5 ± 0.20	11.6 ± 1.09	1.7×10^4
RPR+Pop5+Rpp30 +Rpp21+Rpp29	30	9.50 ± 0.74	0.18 ± 0.04	0.9×10^6

The mean and standard errors for k_{cat} and K_m values were calculated from three independent experiments.

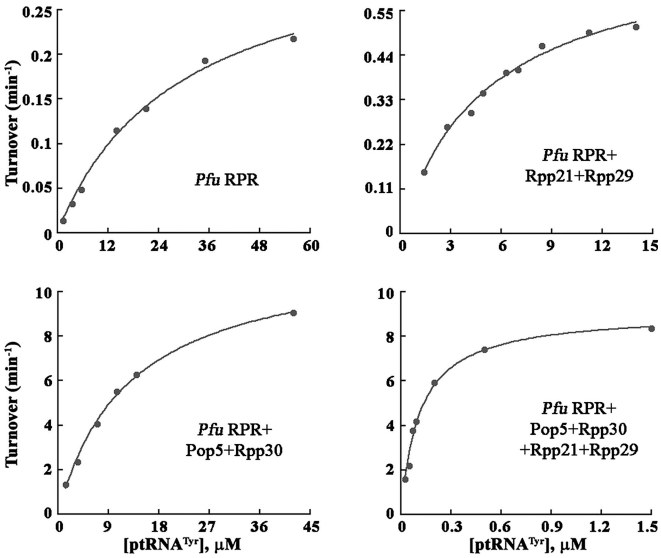

Fig. 3. Michaelis–Menten analysis of partially and fully reconstituted *Pfu* RNase P holoenzymes (see *Supporting Materials and Methods* for details).

Kinetic Studies Using Partially and Fully Reconstituted *Pfu* RNase P Holoenzymes. To gain insights into the contribution of Rpps to *Pfu* RPR catalysis and substrate binding, we determined the steady-state kinetic parameters for ptRNA^{Tyr} processing by *Pfu* RPR, RPR+Pop5+Rpp30, RPR+Rpp21+Rpp29, and RPR+Pop5+Rpp30+Rpp21+Rpp29 (Fig. 3). However, such a comparative study necessitated each catalytic entity to be tested under its optimal conditions. Therefore, we first established the optimal RPR:Rpp ratios and concentrations of NH_4^+/Mg^{2+} for assaying *Pfu* RPR alone or as part of RNP complexes (see *Supporting Materials and Methods* for details).

The k_{cat} exhibited by *Pfu* RPR is enhanced 25-fold by inclusion of the four Rpps (Table 1); this boost parallels the 24-fold increase in k_{cat} of a partially purified native *Mth* RNase P holoenzyme relative to *Mth* RPR alone (21, 31). The K_m exhibited by *Pfu* RPR decreases drastically by 170-fold (from 30.5 μM to 180 nM) in the presence of all four Rpps (Table 1).

Further insights on individual Rpp contributions emerged from examination of partially assembled *Pfu* RNase P holoenzymes. Importantly, Pop5+Rpp30 was able to increase the k_{cat} of RPR by ≈30-fold similar to the effect elicited by all four Rpps. As anticipated from this result Rpp21+Rpp29 hardly impacted the k_{cat} value (a change of only 1.6-fold). It is notable that addition of either Pop5+Rpp30 or Rpp21+Rpp29 to RPR resulted in 3- or 5-fold decrease in K_m, respectively.

Magnesium Requirement for Reactions Catalyzed by Partially and Fully Reconstituted *Pfu* RNase P Holoenzymes. Metal ions play vital roles in RNA structure and catalysis. In a postulated reaction mechanism for RNase P, a hydrated Mg^{2+} ion is believed to generate the hydroxide nucleophile that performs an S_N2 in-line attack on the scissile phosphodiester linkage in the ptRNA substrate (2). Because previous reports indicated that some archaeal RPRs (including *Pfu* RPR) required 300 mM Mg^{2+} even for weak catalytic activity (21) in contrast to the native holoenzymes that only needed 5–30 mM Mg^{2+} (22, 31), we entertained the idea that different Rpp combinations with *Pfu* RPR might require different Mg^{2+} concentrations for optimal activity. Such a premise was not considered in earlier studies (22, 23). Indeed, there is a decrease in optimal [Mg^{2+}] with an increase in the protein complexity of the reconstituted *Pfu* RNase P (Table 1; Fig. 8, which is published as supporting information on the PNAS web site). Whereas the optimal [Mg^{2+}] for *Pfu* RPR-mediated catalysis is 500 mM, this requirement is decreased to 120 and 30 mM when *Pfu* RPR is reconstituted with two and four Rpps, respectively.

Identification of the Catalytic Domain of *Pfu* RPR. The secondary structure model obtained from phylogenetic covariation analysis of many archaeal RPR sequences identified the existence of conserved nucleotides that might constitute its catalytic core (2, 7, 34, 35). We decided to test whether this conserved core in archaeal RPR is sufficient to support catalysis by using a *Pfu* RPR deletion derivative, whose design was based on inferences from bacterial RNase P studies (36–38). Bacterial RPRs are composed of two independently folding units: the specificity (S) and catalytic (C) domains, with the latter capable of independent catalysis in the presence of the Rpp (36–38). The nucleotides in the S-domain of bacterial RPR that recognize the T stem-loop of the ptRNA substrate were identified by an innovative circular permutation analysis coupled with dephosphorylation strategy (39) and by footprinting/photo-crosslinking studies (4, 7, 40). Recent structural studies indicate that these interactions might play a role in precisely orienting the substrate for cleavage by the C-domain (41, 42). In the secondary structure model of *Pfu* RPR, the P7-P10 four-way junction and adjacent loop regions (Fig. 4*A*) resemble the S-domain of bacterial RPR and suggests a similar function in ptRNA binding but not cleavage. We therefore constructed *Pfu* RPRΔ64–222 (Fig. 4*B*), a circularly permuted deletion derivative of *Pfu* RPR (i.e., Cp223–330+1–63), in which the S-domain (from nucleotides 64 to 222) is deleted while leaving intact the highly conserved C-domain.

Indeed, *Pfu* RPRΔ64–222, bereft of the S-domain, forms a functional holoenzyme when reconstituted with the *Pfu* Rpps (Fig. 4*C*, lane 12), although its turnover number is ≈40-fold lower than the holoenzyme reconstituted with *Pfu* RPR (data not shown); *Pfu* RPRΔ64–222 was assayed for 40 min at 55°C in 50 mM Tris-acetate (pH 7.5), 120 mM $Mg(OAc)_2$ and 400 mM NH_4OAc. This deletion derivative either alone or in combination with a single Rpp did not display any activity (data not shown). Because we had already established that the full-length *Pfu* RPR could assemble with either Pop5+Rpp30 or Rpp21+Rpp29 to form a functional (although partial) RNase P holoenzyme (Fig. 2), we investigated how *Pfu* RPRΔ64–222 would fare with these Rpp pairs. We found that *Pfu* RPRΔ64–222 was able to functionally assemble only with the Pop5+Rpp30 combination (Fig. 4*C*, lane 4), and that this activity remained unchanged upon addition of Rpp21+Rpp29 (Fig. 4*C*, lanes 4 versus 12).

Mapping the Binding Sites of the Pop5+Rpp30 Complex on the C-Domain of *Pfu* RPR. Because RNase T1 cleaves 3′ to unpaired guanines, an examination of the RNase T1-digestion patterns of *Pfu* RPR in the absence and presence of the Rpps is expected to reveal at least a few RNA-protein interaction sites in *Pfu* RNase P. Although technical problems complicated footprinting experiments with the full-length *Pfu* RPR, the smaller C-domain-containing RPRΔ64–222 is better behaved in solution and was used in the mapping experiments reported here. Partial digestion of RPRΔ64–222 with RNase T1 was carried out at 55°C under conditions determined to be optimal for *Pfu* RNase P activity.

Upon binding to Pop5+Rpp30, but not Rpp21+Rpp29, nucleotides in L3, P4, L15, J15/2 and J2/4 of *Pfu* RPR displayed decreased susceptibility to RNase T1 (Fig. 4*D*, lanes 3 and 5). In contrast to the 3′ strand of L15, Gs in the 5′ strand are not protected. Although P6 seems to be protected, it is more likely that it is metastable in the absence of Rpps and that it becomes double-stranded in the presence of Pop5+Rpp30 (Fig. 4*D*, lanes 1 and 5).

In the absence of RNase T1, we observed that certain regions in *Pfu* RPR become more susceptible to cleavage (likely Mg^{2+}-induced) upon binding to Pop5+Rpp30 (Fig. 4*D*, lane 6 versus lane 2). Interestingly, these positions are proximal to the nucleotides that

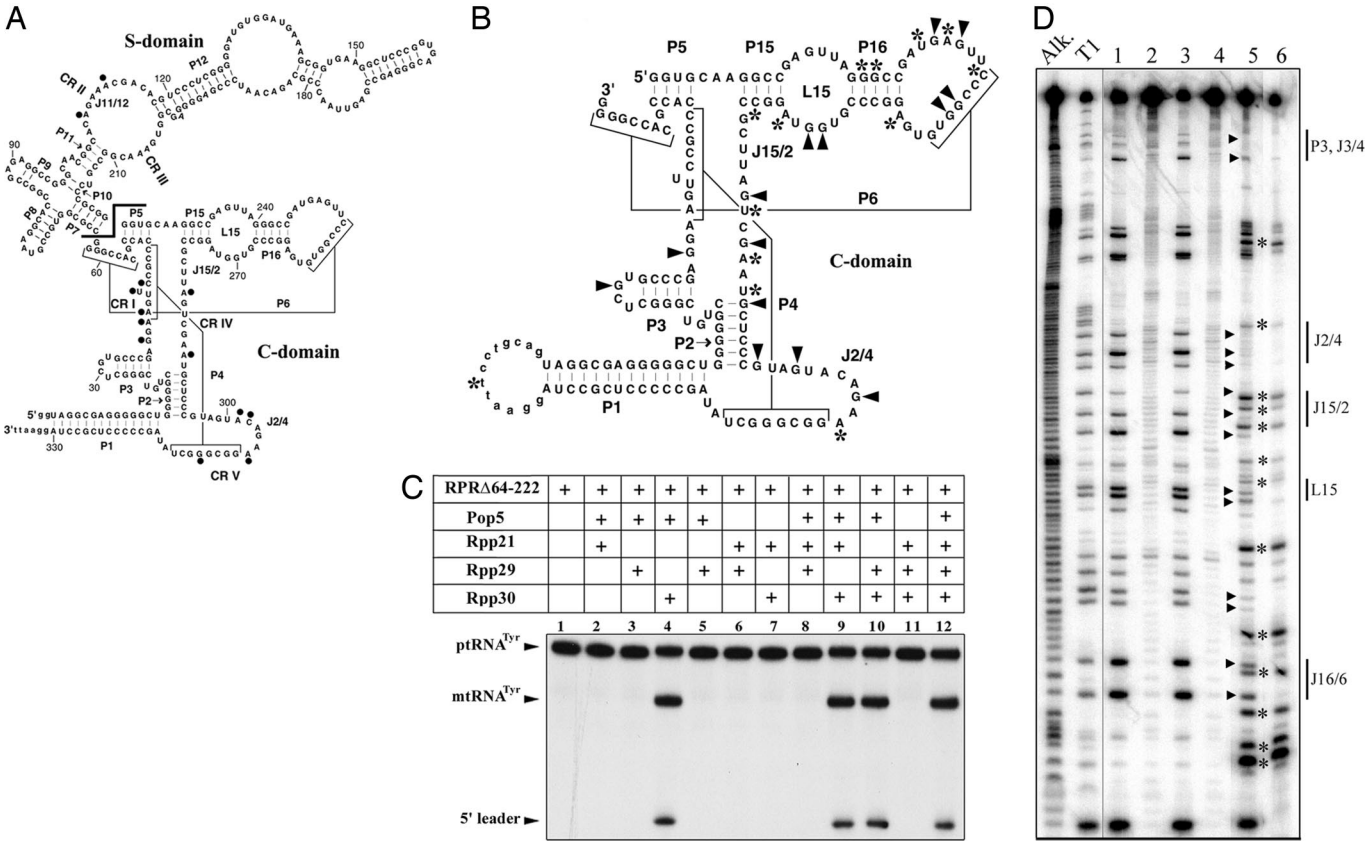

Fig. 4. Identification of a pared down, mini-*Pfu* RNase P. (*A* and *B*) Secondary structure models of *Pfu* RPR and RPRΔ64–222 based on comparative sequence analysis (35). The lowercase letters at the 5′ and 3′ ends represent nucleotides not present in the native *Pfu* RPR. Paired helices (P1, P2, etc.) are numbered according to the *E. coli* RPR nomenclature; the linker joining two helices P15 and P2 is termed J15/2, and the loop that caps the end of a helix P3 is called L3 (50). A black filled circle indicates a universally conserved nucleotide in RPRs from all three domains of life. Unpaired Gs that are protected from RNase T1 are indicated with filled arrows. Asterisks indicate sites of Mg^{2+}-induced cleavage that occur upon binding to Pop5+Rpp30. (*C*) Reconstitution of RNase P activity by using *Pfu* RPRΔ64–222 (500 nM) and various combinations of Rpps (5 μM). (*D*) RNase T1-footprinting analysis of *Pfu* RPRΔ64–222. 5′-end-labeled *Pfu* RPRΔ64–222 either alone, with Rpp21+Rpp29, or with Rpp30+Pop5 was incubated in the presence (lanes 1, 3, and 5, respectively) or absence (lane 2, 4, and 6, respectively) of RNase T1. Alk and T1 represent molecular size ladders generated by subjecting the 5′-end-labeled *Pfu* RPRΔ64–222 to alkaline hydrolysis and partial RNase T1 digestion under denaturing conditions, respectively (see *Supporting Materials and Methods* for details).

are protected from cleavage by RNase T1 (Fig. 4 *B* and *D*). Because Rpps lower the RPR's Mg^{2+} requirement (Table 1 and Fig. 8), changes in metal-ion binding at or around the Rpp-binding sites are likely and these cleavages might reflect the same.

Results from phosphorothioate and hydroxyl radical-mediated footprinting experiments indicate that the bacterial Rpp is proximal to P3, P4, J18/2, and J2/4 (located in conserved regions I, IV and V) in its cognate RPR (17, 43) akin to the footprint of *Pfu* Pop5+Rpp30 on *Pfu* RPR. The conserved nucleotides in these regions have been shown by different biochemical approaches to participate in substrate and Mg^{2+} binding (4). In three-dimensional models of the bacterial RPR/RNase P-ptRNA complex (41–43), these regions are proximal to the ptRNA acceptor stem and cleavage site.

Discussion

***In Vitro* Reconstitution of *Pfu* RNase P.** In this study, we have optimized the conditions for reconstituting the *Pfu* RNase P holoenzyme from its constituent RNA and four protein subunits and demonstrated that this enzyme can perform multiple turnover, an important consideration for any biological catalyst. Although the *Pho* RNase P holoenzyme has been reconstituted (22), steady-state kinetic parameters were not reported. Despite differences in assay conditions (including the substrate used), the k_{cat} of 10–12 min^{-1} that we calculated for the *in vitro* reconstituted *Pfu* RNase P is only a few fold lower than those reported for the native RNase P holoenzymes purified from archaeal sources (≈34–53 min^{-1}; ref. 31) and yeast (≈72 min^{-1}; ref. 44). The K_m value of 180 nM for processing of $ptRNA^{Tyr}$ by reconstituted *Pfu* RNase P compares reasonably with 68 and 34 nM reported for cleavage of *Bacillus subtilis* $ptRNA^{Asp}$ by native *Mja* and *Mth* RNase P, respectively (31). The *in vitro* reconstituted *Pfu* RNase P has a $k_{cat}/K_m \approx 10^6\ M^{-1}\cdot s^{-1}$; in comparison, the partially purified native *Mth* and *Mja* RNase P holoenzymes exhibited $\approx 10^7\ M^{-1}\cdot s^{-1}$.

We list below a few reasons why further improvements in both the k_{cat} and K_m values of *in vitro* reconstituted *Pfu* RNase P may be achievable. First, variations in the ptRNA substrate used or assay conditions [such as inclusion of appropriate polyamines (1)] merit consideration. In fact, we recently found ptRNA substrates that are processed by *Pfu* RNase P with either a 2.5-fold higher k_{cat} or a 4-fold lower K_m than $ptRNA^{Tyr}$ (data not shown). Whereas our preliminary trials proved that spermidine does not alter the k_{cat} of *Pfu* RNase P, we have not yet examined the branched polyamines [e.g., tetrakis (aminopropyl) ammonium] that are found in *Pyrococcus* (45). Second, the recombinant proteins purified after overexpression in *E. coli* may not be completely refolded (as in their native environment) or have the archaeal posttranslational modifications. Lastly, additional protein subunit(s) might be present in archaeal RNase P and the four Rpps we have used might be an incomplete set. In this regard, it is interesting that addition of the

putative *Pho* L7Ae ribosomal protein (a homolog of Rpp38, a human RPP) to *Pho* RPR+Rpp21+Rpp29+Rpp30+Pop5, elevated the optimal temperature for activity from 55°C to 70°C (46). However, there is currently no evidence that L7Ae is associated with a native archaeal RNase P holoenzyme.

Hierarchical Assembly of *Pfu* RNase P. Two different ternary complexes made up of the full-length RPR and an interacting pair of Rpps (RPR+Rpp21+Rpp29 and RPR+Pop5+Rpp30) constitute minimal functional RNPs, as reflected in their higher k_{cat}/K_m values and lower optimal Mg^{2+} concentrations compared with the reaction catalyzed by the RPR alone. These ternary complexes could serve as nucleating intermediates *en route* to assembly of the complete holoenzyme complex of RPR and four Rpps. Changes in the substrate-binding and or cleavage rates of these partially reconstituted *Pfu* RNase P holoenzymes result upon their assembly with the remaining Rpps (Table 1). Because the addition of a third Rpp to a preformed ternary complex of RPR + 2 Rpps has only a modest effect on activity (Fig. 2 and data not shown), interacting protein subunit pairs seem to be the most significant RPR activators. Although these Rpp heterodimers might form on the RNA scaffold, their association before binding is definitely possible.

Whereas these partially active core RNP complexes (RPR+Rpp21+Rpp29 and RPR+Pop5+Rpp30) were not identified in two earlier reports on archaeal RNase P (including ours on *Mth*; refs. 22 and 23), most likely because of the use of suboptimal substrate and Mg^{2+} concentrations in the assay, they are consistent with results of recent studies on archaeal RNase P. First, these pair-wise interactions were predicted by yeast two-hybrid analyses (47, 48). Second, NMR spectroscopic analyses of the *Pfu* Rpp21+Rpp29 and Pop5+Rpp30 complexes revealed significant chemical-shift perturbations in the heteronuclear sequential quantum correlation (HSQC) spectrum of each Rpp upon addition of its partner, indicating strong macromolecular interactions within the pairs and formation of the heterodimers in the absence of *Pfu* RPR (29, 49). Lastly, the *Pho* Pop5-Rpp30 heterodimer was crystallized in an effort to solve the structure of *Pho* Pop5 (30).

Assembly of the *Pfu* RNase P holoenzyme is not an all or none situation where the RNA has to simultaneously bind all four Rpps. It remains to be proven whether the partial (functional) assemblages observed in *Pfu* RNase P represent common intermediates during hierarchical assembly of archaeal/eukaryal RNase P holoenzymes. In this regard, it is notable that weak activity was observed when human RPR was reconstituted with human Rpp21 and Rpp29 (24).

Role of Protein Cofactors/Subunits in *Pfu* RNase P Catalysis. Bacterial Rpp aids its cognate RPR by increasing the (*i*) affinity of the catalytic RNA moiety for the ptRNA substrate (in large part because of a binding pocket that accommodates the ptRNA leader), (*ii*) rate of cleavage, and (*iii*) affinity for Mg^{2+} (13–19). Results from this study indicate that bacterial and archaeal Rpps might employ similar solutions to facilitate RNA catalysis.

Although k_{cat} and K_m values do not shed light on the kinetic scheme for *Pfu* RNase P, some inferences on the role of Rpps can be drawn. First, the fully reconstituted *Pfu* RNase P (i.e., *Pfu* RPR+Pop5+Rpp30+Rpp21+Rpp29) exhibits a $k_{cat}/K_m \approx 10^6$ $M^{-1}\cdot s^{-1}$, which is ≈50-, 560-, and 4285-fold higher than the value obtained in reactions catalyzed by *Pfu* RPR+Pop5+Rpp30, *Pfu* RPR+Rpp21+Rpp29, and *Pfu* RPR, respectively (Table 1); clearly, the overall catalytic efficiency increases with protein complexity. Second, the Pop5+Rpp30 pair (but not Rpp21+Rpp29) can enhance the k_{cat} of RPR to that observed with all four Rpps. Because k_{cat} sets a lower limit on the first-order rate constants for steps subsequent to substrate binding, the Pop5+Rpp30 pair must play a vital role in cleavage and/or product release. Third, among all four Rpps, both nucleating Rpp pairs have the ability to decrease the K_m value (≈3- or 5-fold) although there is a significant synergism (170-fold) when both pairs are present. A comparison of K_m values, which are apparent dissociation constants, exhibited by the RPR in the absence and presence of its Rpps does not permit comments to be made on the effect of Rpps on substrate-binding affinity especially if product release is rate-limiting, a property not ascertained for *Pfu* RNase P. Rate constants for each step in the kinetic scheme need to be determined with the partially and fully reconstituted *Pfu* RNase P holoenzymes to delineate the contribution of the Rpp pairs to the individual steps.

Whereas *Pfu* RPR alone requires 500 mM Mg^{2+} for maximal activity, the two-protein minimal cores (RPR+Rpp21+Rpp29 and RPR+Rpp30+Pop5) function optimally at 120 mM and *Pfu* RNase P reconstituted with all four Rpps exhibits maximum activity at 30 mM Mg^{2+}. Clearly, protein-mediated increase in the affinity of the RNA moiety for Mg^{2+} is being used effectively by archaeal RNase P in a manner reminiscent of its bacterial counterpart (16) and reinforces a recurring theme in protein-assisted RNA catalysis (50).

The similarities in the footprint of bacterial Rpp (17, 43) and *Pfu* Pop5+Rpp30 (Fig. 4) in the C-domains of their respective RPRs is notable for two reasons. First, although only the C-domain was used in the footprinting experiments, many of the nucleotides in *Pfu* RPR that are protected from RNase T1 digestion upon addition of Pop5+Rpp30 lie within universally conserved regions I, IV and V (CR I, IV, and V; Fig. 4), which have been proven to make up the catalytic center in bacterial RPRs (41, 42). This observation together with the 30-fold increase in k_{cat} of the RPR elicited by Pop5+Rpp30 would imply that this Rpp pair is proximal to the cleavage site. Second, given the strikingly similar tertiary structures of *Pfu*/*Pho* Pop5 and bacterial Rpp (29, 30), despite their poor sequence homology and different secondary structure connectivities, the similarity in footprints might suggest parallels in RNA recognition. It was recently demonstrated that *E. coli* Rpp confers uniformity in both binding and catalysis by the RPR on different ptRNAs (including those lacking consensus recognition elements), presumably because of its ability to stabilize the catalytic ES complex to different extents (19). Similar functional roles for archaeal Pop5 merit examination.

Catalysis and RNA–Protein Interactions in *Pfu* RNase P. Conserved structural elements similar to those found in the bacterial RPR have been identified in all archaeal counterparts (7, 35), suggesting a common evolutionary origin for the RNA subunit and a shared catalytic core in all RPRs. Deletion mutants of the *E. coli* RPR (e.g., Δ94–204 or Δ87–241; refs. 36 and 38) that retain the C-domain (P1-P6 + P15–P18) are catalytically active in the presence of the protein cofactor, although with diminished activity and altered substrate specificity. Similarly, *Pfu* RPRΔ64–222, which lacks the S-domain, is functional (Fig. 4*C*), suggesting that the active site resides in the postulated C-domain of *Pfu* RPR and establishes an important, if expected, parallel between bacterial and archaeal RPRs. Moreover, the finding that Pop5+Rpp30, but not Rpp21+Rpp29, can function with *Pfu* RPRΔ64–222 indicates that the C-domain of *Pfu* RPR together with Pop5+Rpp30 represents a pared down, mini-*Pfu* RNase P.

The presence of 13 universally conserved nucleotides in RPRs from all three domains of life (7) supports the possibility of a similar active site and an RNA-dependent catalytic mechanism. However, formation of the catalytic center might depend on different RNA-RNA or RNA-protein interactions in bacterial, archaeal and eukaryal RNase P. The crystal structures of bacterial RPR (without the protein cofactor) reveal how intra-molecular tertiary contacts, acting as struts, might facilitate the exquisite cooperation between the S- and C-domains that allows simultaneous contacts by the two domains with different parts of the ptRNA substrate (41, 42). The absence of these tertiary interactions in archaeal RPRs might explain why they display $\approx 10^3$-fold lower k_{cat}/K_m values (largely because of an increased K_m) compared with their bacterial counterparts. However, because the bacterial and archaeal native ho-

loenzymes exhibit comparable k_{cat}/K_m values of 10^7-10^8 M^{-1}·s^1, the missing inter-domain contacts in archaeal RPRs are likely to be compensated by their cognate Rpps during assembly of the holoenzyme. Although precise details of the archaeal RPR-Rpp interactions remain to be elucidated, results from this investigation suggest that the *Pfu* Rpp21+Rpp29 and Pop5+Rpp30 pairs might interact with the S- and C-domains of the *Pfu* RPR, respectively, and that these interactions enable the inter-domain cooperation required for optimal ptRNA recognition and catalysis.

Summary. Because an archaeal RPR can functionally reconstitute with two different pairs of protein cofactors, mobilizing even two of the four extant protein subunits would have improved the efficiency of a putative ancestral RNase P RNA enzyme. It is possible then that recruitment of protein cofactors by RNA enzymes (like RNase P) could have evolved gradually via RNP intermediates that displayed sequential improvements in catalytic efficiency.

Materials and Methods

Cloning, Overexpression, and Purification of the RNA and Protein Subunits of *Pfu* RNase P. Complete details are provided in *Supporting Materials and Methods*.

***Pfu* RNase P Reconstitution and Assay.** *Pfu* RPR (in water) was folded by incubating for 50 min at 50°C, 10 min at 37°C, and then for 30 min at 37°C in a Mg^{2+}-containing buffer [50 mM Tris·HCl (pH 7.5)/10 mM $MgCl_2$/800 mM NH_4OAc].

Reconstitution experiments were initiated by preincubating folded *Pfu* RPR with either all or a subset of four *Pfu* Rpps in assay buffer [50 mM Tris·HCl (pH 7.5), varying amounts of NH_4OAc and $MgCl_2$] for 5 min at 37°C followed by 10 min at 55°C. The activity was assayed by adding a known concentration of *E. coli* $ptRNA^{Tyr}$, a trace amount of which was internally labeled with [α-^{32}P]GTP. After a defined incubation time at 55°C, the reactions were quenched with urea-phenol dye [8 M urea/0.04% (wt/vol) bromophenol blue/xylene cyanol/0.8 mM EDTA/20% (vol/vol) phenol]. To prevent evaporation losses and aid in rapid temperature equilibration, assays were performed in 0.5-ml thin-walled PCR tubes and a thermal cycler (Eppendorf, Westbury, NY).

Uncleaved $ptRNA^{Tyr}$ and its products (generated by RNase P) were separated by 8% (wt/vol) polyacrylamide/7 M urea gel electrophoresis. The extent of reaction was quantitated by PhosphorImager (Molecular Dynamics) analysis of the polyacrylamide gels. The initial velocity data were converted to turnover numbers and then subjected to Michaelis-Menten analysis by using Kaleidagraph (Synergy Software).

We thank Dr. Mark P. Foster (Ohio State University) and his team members for helpful discussions, Dr. Lien Lai (Ohio State University) for valuable advice on cloning and critical comments on the manuscript, and Dr. Mike Adams (University of Georgia, Athens, GA) for a kind gift of *Pfu* cells and genomic DNA. This work was supported by National Institutes of Health Grant R01 GM067807 (to Mark P. Foster and V.G.), by American Heart Association Pre-Doctoral Fellowships 0315171B (to H.-Y.T.) and 0515218B (to D.K.P.), and by a National Science Foundation Research Experience for Undergraduate Award Supplement (to V.G. for supporting W.K.W.).

1. Guerrier-Takada C, Gardiner K, Marsh T, Pace N, Altman S (1983) *Cell* 35:849–857.
2. Hall TA, Brown JW (2001) *Methods Enzymol* 341:56–77.
3. Jarrous N, Altman S (2001) *Methods Enzymol* 342:93–100.
4. Harris ME, Christian EL (2003) *Curr Op Struct Biol* 13:325–333.
5. Hartmann E, Hartmann RK (2003) *Trends Genet* 19:561–569.
6. Walker SC, Engelke DR (2006) *Crit Rev Biochem Mol Biol* 41:77–102.
7. Evans D, Marquez SM, Pace NR (2006) *Trends Biochem Sci* 31:333–341.
8. Kole R, Altman S (1981) *Biochemistry* 20:1902–1906.
9. Hall TA, Brown JW (2002) *RNA* 8:296–306.
10. Chamberlain JR, Lee Y, Lane WS, Engelke DR (1998) *Genes Dev* 12:1678–1690.
11. Jarrous N (2002) *RNA* 8:1–7.
12. Reich C, Olsen GJ, Pace B, Pace NR (1988) *Science* 239:178–181.
13. Tallsjo A, Kirsebom LA (1993) *Nucleic Acids Res* 21:51–57.
14. Crary SM, Niranjanakumari S, Fierke CA (1998) *Biochemistry* 37:9409–9416.
15. Niranjanakumari S, Stams T, Crary SM, Christianson DW, Fierke CA (1998) *Proc Natl Acad Sci USA* 95:15212–15217.
16. Kurz JC, Fierke CA (2002) *Biochemistry* 41:9545–9558.
17. Buck AH, Kazantsev AV, Dalby AB, Pace NR (2005) *Nat Struct Mol Biol* 12:958–964.
18. Buck AH, Dalby AB, Poole AW, Kazantsev AV, Pace NR (2005) *EMBO J* 24:3360–3368.
19. Sun L, Campbell FE, Zahler NH, Harris ME (2006) *EMBO J* 25:3998–4007.
20. Haas ES, Armbruster DW, Vucson BM, Daniels CJ, Brown JW (1996) *Nucleic Acids Res* 24:1252–1259.
21. Pannucci JA, Haas ES, Hall TA, Harris JK, Brown JW (1999) *Proc Natl Acad Sci USA* 96:7803–7808.
22. Kouzuma Y, Mizoguchi M, Takagi H, Fukuhara H, Tsukamoto M, Numata T, Kimura M (2003) *Biochem Biophys Res Commun* 306:666–673.
23. Boomershine WP, McElroy CA, Tsai HY, Wilson RC, Gopalan V, Foster MP (2003) *Proc Natl Acad Sci USA* 100:15398–15403.
24. Mann H, Ben-Asouli Y, Schein A, Moussa S, Jarrous N (2003) *Mol Cell* 12:925–935.
25. Sidote DJ, Hoffman DW (2003) *Biochemistry* 42:13541–13550.
26. Numata T, Ishimatsu I, Kakuta Y, Tanaka I, Kimura M (2004) *RNA* 10:1423–1432.
27. Takagi H, Watanabe M, Kakuta Y, Kamachi R, Numata T, Tanaka I, Kimura M (2004) *Biochem Biophys Res Commun* 319:787–794.
28. Kakuta Y, Ishimatsu I, Numata T, Kimura K, Yao M, Tanaka I, Kimura M (2005) *Biochemistry* 44:12086–12093.
29. Wilson RC, Bohlen CJ, Foster MP, Bell CE (2006) *Proc Natl Acad Sci USA* 103:873–878.
30. Kawano S, Nakashima T, Kakuta Y, Tanaka I, Kimura M (2006) *J Mol Biol* 357:583–591.
31. Andrews AJ, Hall TA, Brown JW (2001) *Biol Chem* 382:1171–1177.
32. Vioque A, Arnez J, Altman S (1988) *J Mol Biol* 202:835–848.
33. Tsai HY, Lai LB, Gopalan V (2002) *Anal Biochem* 303:214–217.
34. Harris JK, Haas ES, Williams D, Frank DN, Brown JW (2001) *RNA* 7:220–232.
35. Brown JW (1999) *Nucleic Acids Res* 27:314.
36. Guerrier-Takada C, Altman S (1992) *Proc Natl Acad Sci USA* 89:1266–1270.
37. Loria A, Pan T (1996) *RNA* 2:551–563.
38. Green CJ, Rivera-Leon R, Vold BS (1996) *Nucleic Acids Res* 24:1497–1503.
39. Pan T, Loria A, Zhong K (1995) *Proc Natl Acad Sci USA* 92:12510–12514.
40. Nolan JM, Burke DH, Pace NR (1993) *Science* 261:762–765.
41. Torres-Larios A, Swinger KK, Krasilnikov AS, Pan T, Mondragon A (2005) *Nature* 437:584–587.
42. Kazantsev AV, Krivenko AA, Harrington DJ, Holbrook SR, Adams PD, Pace NR (2005) *Proc Natl Acad Sci USA* 102:13392–13397.
43. Tsai HY, Masquida B, Biswas R, Westhof E, Gopalan V (2003) *J Mol Biol* 325:661–675.
44. Xiao S, Day-Storms JJ, Srisawat C, Fierke CA, Engelke DR (2005) *RNA* 11:885–896.
45. Grosjean H, Oshima T (2006) in *Physiology and Biochemistry of Extremophiles*, eds Gerday C, Glansdorff F (Am Soc Microbiol, Washington, DC), in press.
46. Fukuhara H, Kifusa M, Watanabe M, Terada A, Honda T, Numata T, Kakuta Y, Kimura M (2006) *Biochem Biophys Res Commun* 343:956–964.
47. Hall TA, Brown JW (2004) *Archaea* 1:247–254.
48. Kifusa M, Fukuhara H, Hayashi T, Kimura M (2005) *Biosci Biotechnol Biochem* 69:1209–1212.
49. Boomershine WP (2005) PhD thesis (Ohio State University, Columbus).
50. Solem A, Chatterjee P, Caprara MG (2002) *RNA* 8:412–425.